Development of the main olfactory system and main olfactory epithelium-dependent male mating behavior are altered in G_o-deficient mice

Jung-Mi Choi[a], Sung-Soo Kim[a], Chan-Il Choi[a], Hye Lim Cha[a], Huy-Hyen Oh[a,b], Sungho Ghil[c], Young-Don Lee[a,b], Lutz Birnbaumer[d,e,1], and Haeyoung Suh-Kim[a,b,1]

[a]Department of Anatomy, Ajou University School of Medicine, Suwon 16499, South Korea; [b]Department of Biomedical Sciences, The Graduate School, Ajou University School of Medicine, Suwon 16499, South Korea; [c]Department of Life Science, Kyonggi University, Suwon 16227, South Korea; [d]Neurobiology Laboratory, National Institute of Environmental Health Sciences, Research Triangle Park, NC 27709; and [e]Institute of Biomedical Research, School of Medical Sciences, Catholic University of Argentina, C1107AFF Buenos Aires, Argentina

Contributed by Lutz Birnbaumer, August 10, 2016 (sent for review May 5, 2016; reviewed by Cheil Moon and Daniel Storm)

In mammals, initial detection of olfactory stimuli is mediated by sensory neurons in the main olfactory epithelium (MOE) and the vomeronasal organ (VNO). The heterotrimeric GTP-binding protein G_o is widely expressed in the MOE and VNO of mice. Early studies indicated that G_o expression in VNO sensory neurons is critical for directing social and sexual behaviors in female mice [Oboti L, et al. (2014) *BMC Biol* 12:31]. However, the physiological functions of G_o in the MOE have remained poorly defined. Here, we examined the role of G_o in the MOE using mice lacking the α subunit of G_o. Development of the olfactory bulb (OB) was perturbed in mutant mice as a result of reduced neurogenesis and increased cell death. The balance between cell types of OB interneurons was altered in mutant mice, with an increase in the number of tyrosine hydroxylase-positive interneurons at the expense of calbindin-positive interneurons. Sexual behavior toward female mice and preference for female urine odors by olfactory sensory neurons in the MOE were abolished in mutant male mice. Our data suggest that G_o signaling is essential for the structural and functional integrity of the MOE and for specification of OB interneurons, which in turn are required for the transmission of pheromone signals and the initiation of mating behavior with the opposite sex.

heterotrimeric G_o protein | olfactory mucosa | olfactory bulb interneuron | tyrosine monooxygenase | sexual behavior

Pheromones evoke diverse social and sexual behaviors in animals of the same species. In mammals, initial detection of olfactory stimuli is mediated by sensory neurons in the main olfactory epithelium (MOE) and vomeronasal organ (VNO). Early studies indicated that the VNO is largely responsible for the detection of pheromones and the consequent direction of social and sexual behaviors (1). VNO sensory neurons (VSNs) express distinct types of vomeronasal receptors: type 1 (V1Rs) in the apical region and type 2 (V2Rs) in the basal region. These receptors couple, respectively, to G_i and G_o members of the heterotrimeric GTP-binding protein family. It has been suggested that, following ligand binding to V1Rs and V2Rs, the Gβγ subunits released from G_i and G_o activate phospholipase C and increase the intracellular concentration of Ca^{2+}. Ca^{2+} ions induce opening of small Ca^{2+}-activated K^+ (SK3) channels, subsequently activating Ca^{2+}-activated Cl^- channels (CACCs). In the VNO, Gβγ can also directly induce the opening of G protein–activated inward rectifying K^+ (GIRK) channels independently of transient receptor potential cation channel C2 (TRPC2) (2). Because of the VNO's high luminal K^+ concentration (2), opening of SK3 and GIRK channels leads to depolarization of VSNs and transmission of pheromone signals. Targeted deletion of the TRPC2 gene abrogates gender identification and intermale aggression without affecting male-to-female mating behavior in male mice (3, 4). Targeted deletion of the GIRK1 gene partially attenuates mating behavior of the male toward female mice (2). Surgical removal of the VNO does not disrupt sex preference in female hamsters (5) or the mounting behavior of male mice, although it does attenuate the sexual preference of male mice for female mice (6). Taken together, these observations suggest that the VNO plays pivotal roles in identification and discrimination of sex, although preference for the opposite sex may additionally involve non-VNO organs.

Accumulating evidence supports a role for the MOE in preference for the opposite sex and mating initiation. Chemical destruction of the MOE with zinc sulfate abrogates urinary odor preference in female mice (7). In olfactory sensory neurons (OSNs), binding of general odorants to olfactory receptors (ORs) stimulates the OR-coupled heterotrimeric G protein G_{olf}. G_{olf} activates adenylyl cyclase 3 (AC3, encoded by *Adcy3*) and increases the levels of cAMP. As a result, cyclic nucleotide-gated α2 channels (CNGA2, encoded by *Cnga2*) are opened, and OSNs become depolarized. Targeted deletion of CNGA2 (8) or AC3 (9) genes, which are expressed in the MOE but not in the VNO, disrupts the preference for female urine odors in male mice and impairs male–female mating behavior, suggesting that the MOE has a role in pheromone detection and mating behavior. Taken together, these observations indicate that the MOE may be essential for initiation of pheromone-evoked mating behavior and preference for the opposite sex. Mice deficient in G_{olf} are anosmic

Significance

Early studies indicated that two olfactory systems in mammals play distinct roles: The main olfactory system detects general odorants, and the accessory olfactory system detects pheromones. Using heterotrimeric G_o protein-deficient mice, we show that pheromone detection by the main olfactory system is necessary for the initiation of mating behavior toward the opposite sex and that G_o plays a key role in this process by regulating the development of the main olfactory epithelium and the differentiation of dopaminergic interneurons in the olfactory bulb. Our findings provide the basis for identifying pheromone receptors in the main olfactory system and for understanding the hyposmia found in Parkinson's disease, in which the number of inhibitory dopaminergic interneurons is increased in the olfactory bulb.

Author contributions: J.-M.C., L.B., and H.S.-K. designed research; J.-M.C., C.-I.C., H.L.C., H.-H.O., and S.G. performed research; J.-M.C., S.-S.K., Y.-D.L., L.B., and H.S.-K. analyzed data; and J.-M.C., L.B., and H.S.-K. wrote the paper.

Reviewers: C.M., Daegu Gyeongbuk Institute of Science and Technology; and D.S., University of Washington.

The authors declare no conflict of interest.

Freely available online through the PNAS open access option.

[1]To whom correspondence may be addressed. Email: Birnbau1@gmail.com or hysuh@ajou.ac.kr.

This article contains supporting information online at www.pnas.org/lookup/suppl/doi:10.1073/pnas.1613026113/-/DCSupplemental.

and fail to thrive because of their inability to suckle. However, the rare G_{olf} homozygotes that survive to sexual maturity are fertile and mate (10). Thus, it remains to be elucidated why AC3- and CNGA2-deficient mice, unlike G_{olf} mutant mice, lose the preference for the opposite sex and which G proteins regulate this signaling pathway in OSNs of the MOE.

In OSNs, the expression of $G\alpha_{i2}$, α subunit of G_{i2}, is largely absent from the olfactory bulb (OB), with the exception of neurons in the medial part that receive incoming axons from a small subpopulation of OSNs (11). Targeted deletion of $G\alpha_{i2}$ disrupts the aggressive behavior of males without affecting the preference for the opposite sex (12). By comparison, $G\alpha_o$, α subunit of G_o, is widely expressed in OSNs of the MOE (11). Attempts have been made to delete $G\alpha_o$ in the MOE using Cre recombinase expressed under the control of the olfactory marker protein (OMP) gene promoter. However, conditional knockout of $G\alpha_o$ (c*Gnao*$^{-/-}$) using OMP-Cre results in the loss of $G\alpha_o$ expression specifically in the VNO, apparently leaving expression in the MOE intact (13). Such a VNO-restricted deficiency of $G\alpha_o$ disrupts only the aggressive behavior of males without affecting the preference for the opposite sex (13, 14). Collectively, these observations suggest that the MOE plays a role in detecting pheromones that trigger sexual behaviors such as preference for the opposite sex and initiation of sexual activity. They also raise the question of which G protein conveys pheromone signaling in the MOE.

We show here that male $G\alpha_o$-knockout (*Gnao*$^{-/-}$) mice, which lack $G\alpha_o$ in both the MOE and VNO, fail to develop a preference for female urine odors and are unable to engage in mounting behavior with estrous females. Although mutant mice exhibited a reduction in MOE mass, they retained an ability to detect general odorants comparable to that of WT (*Gnao*$^{+/+}$) mice. Surprisingly, the number of tyrosine hydroxylase (TH)-positive interneurons was increased in the OB of *Gnao*$^{-/-}$ mice, whereas the number of calbindin (CB)-positive interneurons was reduced. Our data indicate that G_o plays important roles in the regulation of neurogenesis and cell-type specification in the main olfactory system and thus in the detection of pheromones. They also implicate a G_o-mediated sensory contribution of the MOE to the preference for the opposite sex and mating initiation.

Results

$G\alpha_o$ Ablation Leads to an Altered MOE. *Gnao*$^{-/-}$ mice were obtained by crossing heterozygous *Gnao*$^{+/-}$ mice as previously described (15). These mice have a low birth rate and rarely survive to adulthood because of severe neurological deficits, including hyperactivity and seizures. We compared the overall structure of the MOE and VNO in adult *Gnao*$^{+/+}$ and *Gnao*$^{-/-}$ mice (Fig. 1 *I* and *J*). H&E staining of corresponding coronal sections of the adult mouse brain revealed that the sensory epithelia of the MOE and VNO were atrophied in *Gnao*$^{-/-}$ mice compared with *Gnao*$^{+/+}$ mice (Fig. 1 *A* and *B*). Immunohistofluorescence analyses of *Gnao*$^{+/+}$ mice showed that OMP and neuron-specific β-III tubulin (Tubb3) are present throughout the VNO sensory epithelium (VNE), as previously reported (16). $G\alpha_o$ protein is also present in VSNs as well as at the luminal surface containing the microvilli that extend from these neurons (Fig. 1 *C* and *E*). Such immunoreactivity was not detected in *Gnao*$^{-/-}$ mice, validating the specificity of the immunohistological approach. The posterior accessory olfactory bulb (AOB), which contains incoming axons from the basal VNO, was also atrophied in *Gnao*$^{-/-}$ mice (Fig. S1), consistent with previous observations that $G\alpha_o$ ablation results in degeneration of the basal layer of the VNE and the posterior AOB (13, 17). In the MOE of adult *Gnao*$^{+/+}$ mice, $G\alpha_o$ was detected in most cells along the apical–basal axis, including OMP$^+$ mature OSNs, Tubb3$^+$ immature OSNs, and sustentacular cells (Fig. 1 *D* and *F*). Because $G\alpha_o$ protein is highly targeted to the plasma membrane, whereas the OMP protein is cytosolic, it was necessary to locate $G\alpha_o$ and OMP expression precisely. Postnatal

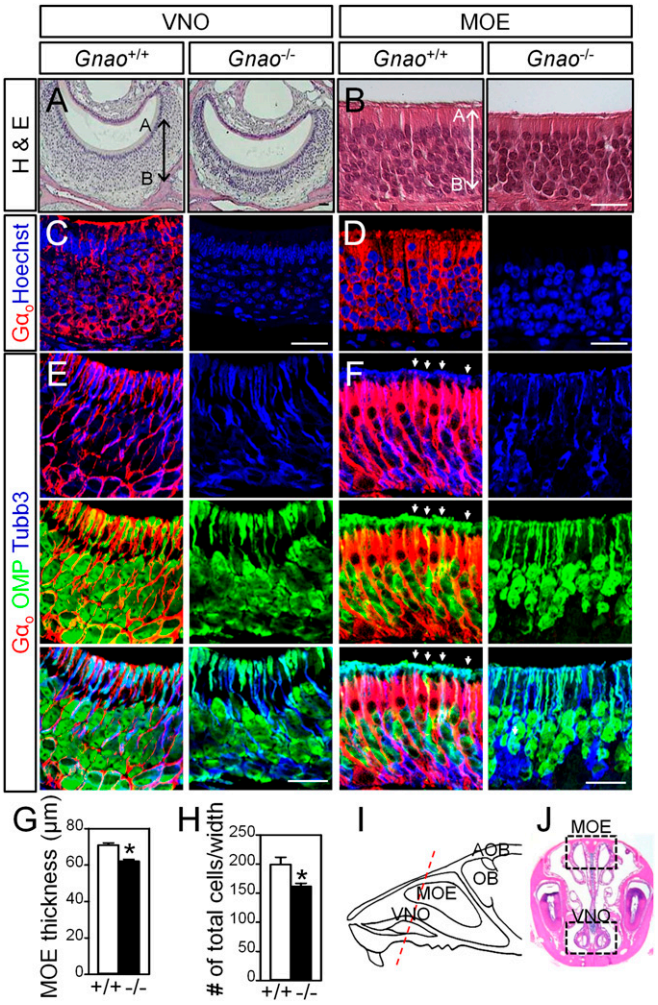

Fig. 1. Defective development of the neuronal layer of the MOE and basal VNO in *Gnao*$^{-/-}$ mice. (*A* and *B*) H&E staining of the VNO (*A*) and MOE (*B*) showing the reduced thickness of the neuronal cell layer (A–B, apical–basal) in *Gnao*$^{-/-}$ mice compared with *Gnao*$^{+/+}$ mice. (*C* and *D*) Immunostaining showing $G\alpha_o$ enrichment (red) in the basal VNO (*C*) and its wide distribution in the apical and basal MOE (*D*) in the WT mice. Nuclear staining (Hoechst; blue) revealed reduced cell density in the VNO and MOE of the mutant. (*E* and *F*) Immunostaining of $G\alpha_o$ (red), OMP (green), and Tubb3 (blue). $G\alpha_o$ was expressed in OMP$^+$ and Tubb3$^+$ VSNs (*E*), as well as in most cells of the MOE, including mature OMP$^+$ OSNs, immature Tubb3$^+$ OSNs, and apical sustentacular cells (*F*). Arrowheads indicate the dendritic knobs of OSNs. (Scale bars: 20 μm.) (*G* and *H*) The thickness of the neuronal layer was measured (*G*), and the total number of cells (*H*) were counted in an area with a width of 250 μm. $n = 34$ sections from three *Gnao*$^{+/+}$ mice and 28 sections from three *Gnao*$^{-/-}$ mice. Data are means ± SEM; $^*P < 0.05$ vs. *Gnao*$^{+/+}$. (*I* and *J*) Sagittal (*I*) and coronal (*J*) views of the mouse nasal cavity showing the two separate olfactory systems, MOE–OB and VNO–AOB.

day 7 (P7) mice, in which the nasal bone was fully calcified and nose regions containing the MOE and VNO was cryosectioned without a decalcification process. In situ hybridization with a *Gnao*-antisense RNA probe revealed wide expression of *Gnao* mRNA in the entire MOE along the apical–basal axis except in cells adjacent to the lamina propria, confirming the immunohistochemical results (Fig. S2*B*). Immunohistochemistry using an anti-OMP antibody revealed that the presence of OMP was limited to the apical region (Fig. S2*C*). Again, such *Gnao* mRNA signals were not detected with *Gnao*-sense RNA probes, validating the specificity of our approach (Fig. S2, *Upper*). Importantly, $G\alpha_o$ ablation reduced MOE thickness by ~13% and total cell number

NEUROSCIENCE

by ~20% (Fig. 1 *G* and *H*). These results thus indicate that G_o is essential for maintenance not only of the VNE, but also of the MOE.

$G\alpha_o$ Ablation Impairs MOE Neurogenesis. We next investigated how $G\alpha_o$ ablation resulted in MOE atrophy. TUNEL analyses revealed a 4.5-fold increase in the number of apoptotic cells in the MOE of adult *Gnao*$^{-/-}$ mice (Fig. 2 *A* and *E*). In addition, the number of proliferating cell nuclear antigen (PCNA)-positive proliferating cells, mammalian achaete-scute homolog 1 (Mash1)-positive progenitor cells, and sex determining region Y-box 2 (Sox2)-positive basal progenitor cells in the MOE were significantly reduced in *Gnao*$^{-/-}$ mice (Fig. 2 *B–D* and *F*). The number of Sox2$^+$ apical sustentacular cells, all of which originate from a common progenitor (18), was also reduced in the MOE of *Gnao*$^{-/-}$ mice (Fig. 2 *D* and *F*). These results thus indicate that the overall reduction in the size of the MOE induced by $G\alpha_o$ ablation was the result of the combined effects of reduced neurogenesis and increased cell death. Consistent with these findings, the olfactory nerve layer (ONL) of the OB, which comprises projecting axons of OMP$^+$, neural cell adhesion molecule (NCAM)-positive and $G\alpha_o^+$ OSNs, was thinner in the mutant (Fig. S3). In contrast, microtubule-associated protein 2 (MAP2) staining in the glomerular layer (GL), where dendrites of mitral cells make synaptic contact with incoming OSN axons, and in the external plexiform layer (EPL) of the OB appeared unaffected in *Gnao*$^{-/-}$ mice. These observations suggest that the structural changes of the MOE induced by the loss of $G\alpha_o$ may not extend beyond the GL.

$G\alpha_o$ Ablation Alters Cell-Type Specification in the OB. Neurotransmission between pre- and postsynaptic fibers in the GL of the OB is extensively modulated by periglomerular interneurons that exclusively express tyrosine TH, CB, or calretinin (CR) (19). Deprivation

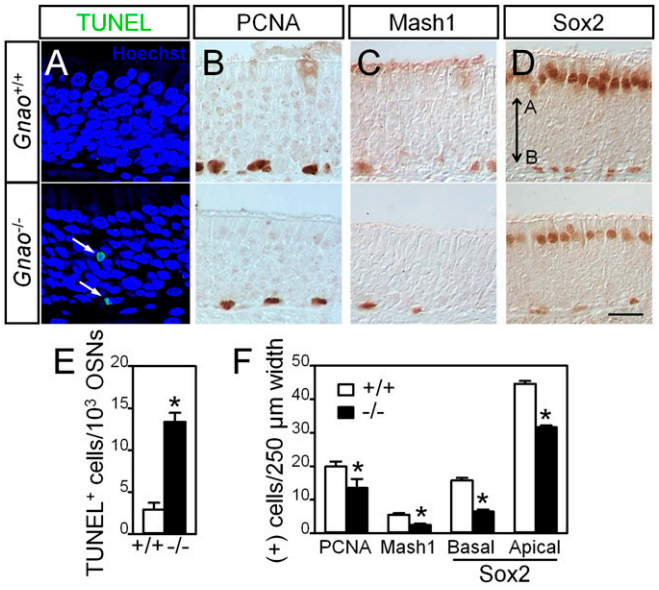

Fig. 2. Increased apoptosis and reduced neurogenesis in the MOE of *Gnao*$^{-/-}$ mice. (*A*) TUNEL staining of apoptotic cells (green; arrows) in the MOE of *Gnao*$^{+/+}$ and *Gnao*$^{-/-}$ mice. Nuclear staining (Hoechst dye; blue) revealed condensed nuclei in the *Gnao*$^{-/-}$ MOE. (*B–D*) Immunostaining of PCNA$^+$ proliferating cells (*B*), Mash1$^+$ progenitor cells (*C*), and Sox2$^+$ basal progenitor cells and apical sustentacular cells (*D*) in the MOE of *Gnao*$^{+/+}$ and *Gnao*$^{-/-}$ mice. (Scale bar: 20 μm.) (*E*) The number of TUNEL$^+$ cells per 1,000 OSNs in the MOE. Data are means ± SEM; *Gnao*$^{+/+}$: n = 2,850 cells in 25 sections from two mice; *Gnao*$^{-/-}$: n = 2,475 cells in 25 sections from two mice. (*F*) The number of immunoreactive cells in each section in an area with a width of 250 μm. Data are means ± SEM; *$P < 0.05$ vs. *Gnao*$^{+/+}$ mice; *Gnao*$^{+/+}$: n = 26–39 sections from three mice; *Gnao*$^{-/-}$: n = 26–30 sections from three mice.

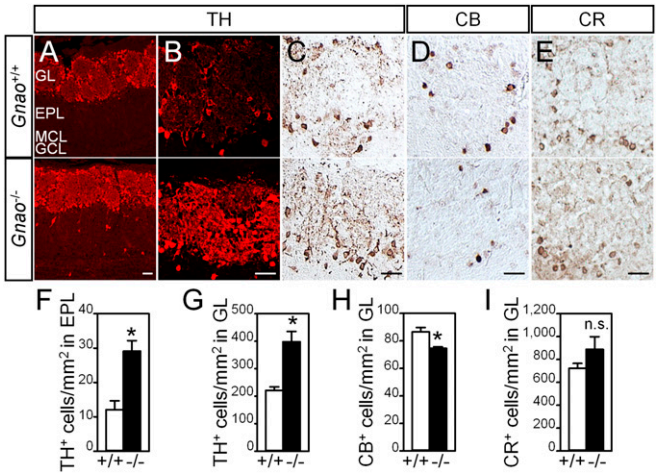

Fig. 3. Increased number of TH$^+$ interneurons in the OB of *Gnao*$^{-/-}$ mice. (*A–C*) Immunofluorescence (*A* and *B*) and immunohistochemical (*C*) staining for TH in the OB of *Gnao*$^{+/+}$ and *Gnao*$^{-/-}$ mice. GCL, granule cell layer; MCL, mitral cell layer. (*D* and *E*) Immunohistochemical staining for CB (*D*) and CR (*E*) in the OB. (Scale bars: 20 μm.) (*F–I*) Numbers of interneurons in the OB. Data are means ± SEM; *$P < 0.05$ vs. *Gnao*$^{+/+}$ mice; n.s., not significant; *Gnao*$^{+/+}$: n = 9–12 sections from two mice; *Gnao*$^{-/-}$: n = 8–13 sections from two mice.

of presynaptic input from the ONL in rodents, either by treatment with zinc sulfate or by naris occlusion, was previously shown to reduce both TH expression and dopamine levels in the GL of the OB (20, 21), whereas naris reopening resulted in the generation of new TH$^+$ interneurons (22). We therefore expected that the reduced thickness of the ONL in the OB of *Gnao*$^{-/-}$ mice would be associated with a reduction in TH expression or a reduced number of TH$^+$ periglomerular cells. However, we found that the number of TH$^+$ interneurons was actually increased ~1.9-fold in the GL and ~2.5-fold in the EPL of *Gnao*$^{-/-}$ mice (Fig. 3 *A–C*, *F*, and *G*). One possible explanation for these results is that OB progenitor cells might tend to differentiate toward TH$^+$ interneurons in the absence of $G\alpha_o$, in which case the number of CB$^+$ interneurons, which differentiate from the same progenitor cells. Indeed, we found that the number of CB$^+$ interneurons in the GL was reduced in the mutant by ~13% (Fig. 3 *D* and *H*). In contrast, the number of CR$^+$ interneurons, which arise from a different population of progenitor cells, was not affected by $G\alpha_o$ ablation (Fig. 3 *E* and *I*).

Although the receptors for various neurotransmitters, including glutamate, serotonin, opioids, acetylcholine, and ATP, are thought to be coupled to G_i or G_o, the dopamine type 2 receptor (D2R) has been unambiguously shown to signal mostly, if not exclusively, via G_o (23). In rodents, the embryonic OB contains immature GABA$^+$ progenitor cells that subsequently differentiate into mature TH$^+$ cells (24). We next tested whether the suppression of D2R-activated G_o signaling mimicked the effect of $G\alpha_o$ ablation on the number of TH$^+$ cells generated by OB progenitors. To this end, we isolated OB neurons from WT mice at embryonic day 16.5 (E16.5) and cultured the cells for 1 d in the presence of the D2R antagonist sulpiride to block G_o signaling. Addition of sulpiride did not affect the number of TH$^+$ neurons, and pretreatment with it did not affect the dopamine-induced increase in the number of TH$^+$ cells; treatment with the D2R agonist ropinirole was similarly without effect (Fig. S4). These results suggest that OB progenitor cells at E16.5 are already predisposed to become either TH$^+$ or CB$^+$ neurons in a cell-autonomous manner and that the prospective TH$^+$ or CB$^+$ neurons are not converted to other types of interneurons in response to D2R signaling.

To examine whether the neurochemical phenotypes of OB interneurons are specified at E16.5 by $G\alpha_o$, we analyzed dissociated neuronal cultures prepared from the OB of E16.5 *Gnao*$^{-/-}$ mice or their *Gnao*$^{+/+}$ littermates. Consistent with in vivo results, the

number of TH$^+$ neurons in *Gnao*$^{-/-}$ cultures was increased ~2.2-fold compared with *Gnao*$^{+/+}$ cultures (Fig. 4 *A* and *C*), whereas the number of CB$^+$ neurons was reduced by approximately one-half (Fig. 4 *B* and *D*). These data indicate that more embryonic OB progenitor cells are predisposed to differentiate into TH$^+$ interneurons than into CB$^+$ interneurons in the absence of Gα_o and that G$_o$ therefore may play a pivotal role in regulating the specification of TH$^+$ and CB$^+$ interneurons in the OB.

Gα_o Ablation Impairs Sexual Behavior. We next tested whether Gα_o ablation in the MOE and VNO impairs olfactory sensation, as measured by the hidden food detection test. The latency to finding the hidden food and the total time spent in the vicinity of the food did not differ in *Gnao*$^{-/-}$ and *Gnao*$^{+/+}$ male mice (Fig. 5 *A* and *B*). Thus, the overall function of odor detection was not affected in *Gnao*$^{-/-}$ mice, despite the evident atrophy of the MOE and VNO in these animals. These results suggest that the contribution of G$_o$ to food detection is minimal.

We then examined whether Gα_o ablation affects pheromone detection. *Gnao*$^{-/-}$ mice are born in reduced number, have a high death rate, and manifest increased locomotor activity (15). We therefore designed a noninvasive experiment to test whether male mice are able to smell pheromones in female urine. In this experimental paradigm, soiled bedding from males, estrous females, or anestrous females was randomly placed in three alternate compartments of a five-compartment apparatus, with fresh bedding placed in the two intervening compartments. *Gnao*$^{+/+}$ male mice spent more time in the bedding soiled by estrous females than in the other bedding types and spent the least amount of time in the fresh bedding. In contrast, *Gnao*$^{-/-}$ male mice spent similar amounts of time in all types of bedding, including fresh bedding, thus exhibiting no preference for any compartment (Fig. 5*C*). These results suggest that *Gnao*$^{-/-}$ male mice have lost the ability to detect pheromone cues in female urine, even though their ability to detect food odorants remains intact.

To examine mating behavior, we introduced an unfamiliar estrous WT female mouse that was highly sexually receptive into the home cage of a male mouse. *Gnao*$^{+/+}$ male mice intensively investigated the anogenital area of the female mouse and attempted to mount the female, but *Gnao*$^{-/-}$ males showed little interest in the female, exhibiting a greatly reduced frequency of anogenital investigation and an almost complete absence of mounting behavior (Fig. 5*D*). *Gnao*$^{-/-}$ male mice showed no gross anatomic

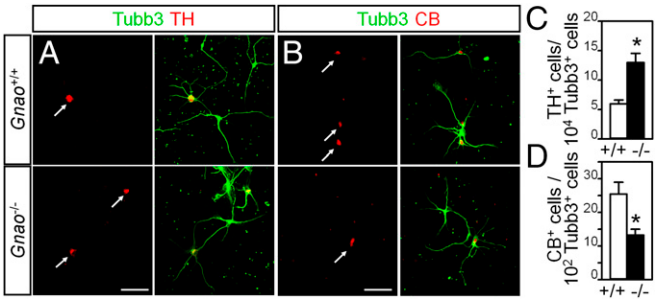

Fig. 4. Increased number of TH$^+$ interneurons in *Gnao*$^{-/-}$ OB neuron cultures. (*A* and *B*) Representative immunofluorescence staining for Tubb3 (green) and TH (red; *A*) or CB (red; *B*) in primary cultured OB neurons from E16.5 *Gnao*$^{+/+}$ and *Gnao*$^{-/-}$ mice. TH or CB immunoreactivity was evident in subsets of Tubb3$^+$ neurons (arrows). (Scale bars: 50 μm.) (*C* and *D*) The number of TH$^+$ neurons per 10,000 Tubb3$^+$ neurons (*C*) or CB$^+$ neurons per 100 Tubb3$^+$ neurons (*D*). TH$^+$ neurons were determined by analyzing a total of 1,779 Tubb3$^+$ neurons from four *Gnao*$^{+/+}$ embryos and 1,176 Tubb3$^+$ neurons from three *Gnao*$^{-/-}$ embryos; CB$^+$ neurons were determined by analyzing 411 Tubb3$^+$ neurons from three *Gnao*$^{+/+}$ embryos and 278 Tubb3$^+$ neurons from *Gnao*$^{-/-}$ embryos. Data are means ± SEM; $^*P < 0.05$ vs. *Gnao*$^{+/+}$.

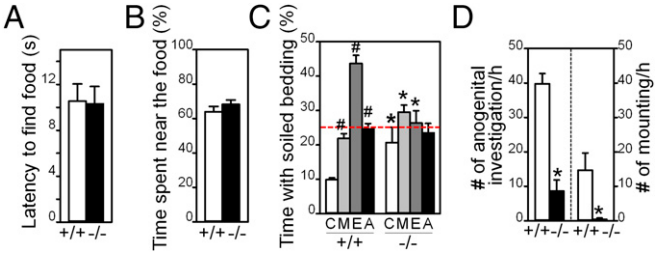

Fig. 5. Impaired sexual behavior and sex partner preference in *Gnao*$^{-/-}$ male mice. (*A* and *B*) Time to find the hidden food (*A*) and the percentage of time spent near the food (*B*) in the hidden food-detection test for male mice. Data are means ± SEM; $n = 10$ for *Gnao*$^{+/+}$ and 10 *Gnao*$^{-/-}$ mice. (*C*) Time spent by *Gnao*$^{+/+}$ and *Gnao*$^{-/-}$ male mice in bedding soiled by males (M), estrous females (E), or anestrous females (A). The time spent in fresh, clean (C) bedding is the average of the time spent in the two compartments. Data are means ± SEM; $^{\#}P < 0.05$ vs. the corresponding value for fresh bedding; $^*P < 0.05$ versus the corresponding value for *Gnao*$^{+/+}$ mice; *Gnao*$^{+/+}$: $n = 8$ mice; *Gnao*$^{-/-}$: $n = 6$ mice. (*D*) The number of anogenital investigations and mounting events with an estrous female for *Gnao*$^{+/+}$ and *Gnao*$^{-/-}$ male mice. Data are means ± SEM; $^*P < 0.05$ versus the corresponding value for *Gnao*$^{+/+}$ mice; *Gnao*$^{+/-}$: $n = 6$ mice; *Gnao*$^{-/-}$: $n = 5$ mice.

defects in reproductive organs, including seminal vesicles, testes, and epididymis (Fig. S5), suggesting that testosterone levels are similar in these mutant mice and *Gnao*$^{+/+}$ males. The lack of anogenital investigation by *Gnao*$^{-/-}$ male mice therefore is not likely attributable to a secondary effect of defective reproductive organs or reduced testosterone levels but rather reflects impaired preference for the opposite sex. Taken together, these results suggest that *Gnao*$^{-/-}$ male mice do not show a sexual partner preference because they lack the ability to detect pheromone cues.

Discussion

Mouse genetic studies have suggested that the MOE–OB and VNO–AOB pathways are essential mediators of pheromone-triggered social and sexual behaviors. Deletion of VNO-specific genes such as *Trpc2* has been found to disrupt gender identification while sparing sex preference (3, 4). By comparison, both preference for the opposite sex and the initiation of sexual behaviors, such as anogenital investigation and mounting, are lost as a result of deletion of the MOE-specific genes *Adcy3* or *Cnga2* (8, 9). Global deletion of the gene encoding Gα_{i2} (*Gnai2*), which is expressed in the apical VNO and anterior AOB (12), or conditional Gα_o knockout (c*Gnao*$^{-/-}$) using an OMP-Cre construct disrupts intermale and maternal aggressive behaviors without affecting sexual behavior (13, 14). We show here that *Gnao*$^{-/-}$ male mice barely investigated the anogenital area of female mice and did not show a preference for bedding soiled by estrous females. They therefore lacked the preference for a female sex partner and largely failed to engage in sexual behavior. Taken together with previous mouse genetic studies, our results suggest that, although both the MOE and VNO detect pheromone signals and trigger mating behavior, the MOE appears to make a greater contribution to the preference for the opposite sex and initiation of sexual behavior, whereas the VNO mediates gender identification (Fig. 6).

Structural alterations were widespread along the apical–basal axis in the MOE of *Gnao*$^{-/-}$ mice, affecting OMP$^+$ OSNs as well as progenitor cells in the basal region and sustentacular cells in the apical region. Nevertheless, food-detection ability appeared normal in the mutant animals, with only pheromone detection being selectively impaired (Fig. 5). General odorants, such as those of food, are detected by canonical OMP$^+$ OSNs in the MOE, and their intracellular signals are transmitted via the α subunit of the G protein G$_{olf}$ and the cAMP signaling cascade (25, 26). Therefore, intact G$_{olf}$ accounts for the normal ability of *Gnao*$^{-/-}$ mice to detect food pellets (Fig. 5 *A* and *B*) but cannot

NEUROSCIENCE

replace the function of G_o in transducing pheromone signals in the MOE. In the early postnatal period between P4 and P7, the expression of $G\alpha_o$ protein or *Gnao* mRNA is widely detected in the MOE, whereas OMP expression, the hallmark of mature OSNs, is limited to the apical region (Figs. S2 and S6). OMP expression is the hallmark of mature OSNs, which extend dendritic knobs to the ciliary layer (27). $G\alpha_o$ was detected in a subset of dendritic knobs in P4 and in adult MOE. Further studies are necessary to elucidate whether the $G\alpha_o$ in dendritic knobs at the ciliary layer functions in pheromone transduction.

Previous studies using an independently generated G_o-deficient mouse model also reported that homozygous-null animals retained the ability to locate food but had lost the specific sense of Nasonov pheromones such as geraniol and citralva (28). Animals in a state of food deprivation will work much harder to obtain food in an operant task than animals fed ad libitum, because hunger modulates the sensitivity to sensory cues associated with food and influences behavioral responses (29). Thus, it is possible that the G_{olf}-driven ability to detect food may be enhanced after food deprivation in G_o-deficient mice. The fact that WT and G_o-deficient mice have a similar ability to locate food may indicate that the neural circuits of hypothalamic neurons that sense energy deficits and induce food seeking and consumption may be functional in the brain-wide absence of G_o. Thus, it is likely that the lack of preference for the opposite sex in *Gnao*$^{-/-}$ males is attributable to the selective failure of pheromone detection. However, we cannot rule out the possibility that neural circuits in other areas that control the initiation of sexual behavior toward the opposite sex are selectively damaged in the absence of G_o.

Our results support a recent study showing that G_{olf} and G_o mediate alternate signaling pathways in an individual OR-expressing OSN in a ligand-selective manner. Applying RNA-sequencing technology to single OSNs, Scholz and colleagues found that G_{olf} and G_o are coexpressed in the same neuron, where they independently activate distinct signaling pathways in a stimulus-dependent manner upon the binding of diverse ligands to the same Olfr73 olfactory receptor (30): $G\alpha_o$ activation leads to an efflux of Cl^- that is independent of canonical pathways, including activation of AC3, increases in Ca^{2+} stemming from extra- or intracellular sources, or phosphatidylinositol 3-kinase–dependent signaling (31); and, as mentioned in the Introduction, G_o-derived $G\beta\gamma$ activates GIRK channels independently of TRPC2. Thus, in the VNO, unlike other sensory organs, SK3, GIRK, and CACC channel activation of its VSNs leads to K^+ influx and Cl^- efflux (2). AC3$^{-/-}$ and *Gnao*$^{-/-}$ mice exhibit similar phenotypes (Fig. 6), and the MOE expresses multiple types of adenylyl cyclases (ACs) including AC2, AC3, and AC4 (32). It would be of interest to elucidate whether G_o activates any of these ACs. Several studies have reported that specialized OSNs express trace amine-associated receptors (33), guanylyl cyclase-D (34), or TRPC2 (35). G_o is found in TRPC2-expressing OSNs in the MOE, some of which do not express AC3 or G_{olf}. It is possible that G_o may regulate pheromone signals in these specialized neurons of the MOE.

Interestingly, most $G\alpha_o$-expressing neurons in the basal MOE were devoid of OMP expression in the P4–7 MOE, whereas most $G\alpha_o$-expressing neurons expressed OMP in the P7 VNE (Fig. S2). Such OMP expression in a subpopulation of $G\alpha_o^+$ cells in the apical MOE during early postnatal periods might cause insufficient deletion of *Gnao* by OMP-driven Cre recombinase in the MOE of OMP-Cre::*Gnao*$^{floxed/floxed}$ (c*Gnao*$^{-/-}$) mice, resulting in a *Gnao*$^{+/+}$ phenotype in the MOE of c*Gnao*$^{-/-}$ mice, as previously surmised (13). Indeed, c*Gnao*$^{-/-}$ mice have been shown to retain WT male sexual preference and mounting behavior (14), as summarized in Fig. 6.

Ablation of $G\alpha_o$ reduced the thickness of the MOE and VNO (Fig. 1). In agreement with a previous report showing increased cell death in the VNO in *Gnao*$^{-/-}$ mice (17), we found that TUNEL$^+$ apoptotic cells were increased in the MOE of *Gnao*$^{-/-}$ mice (Fig. 2), indicating that G_o is critical for neuronal cell survival in both the MOE and VNO. We also found that the numbers of Mash1$^+$ and Sox2$^+$ basal cells, as well as PCNA$^+$ proliferating cells, were reduced in the MOE of *Gnao*$^{-/-}$ mice. Taken together, these data indicate that G_o signals are necessary not only for the survival of OSNs but also for the neurogenesis of MOE neurons.

TH$^+$ dopaminergic periglomerular interneurons inhibit synaptic transmission between OSNs and mitral cells in the OB by releasing dopamine and GABA. It has been found that the number of periglomerular TH$^+$ neurons is markedly increased in pathological conditions such as Alzheimer's disease and Parkinson's disease (36). Olfactory dysfunction is considered a reliable marker of these diseases that precedes the typical clinical manifestations by many years (37); however, the mechanisms underlying this association are poorly understood. We have now shown that $G\alpha_o$ ablation impairs pheromone detection and increases the number of TH$^+$ OB interneurons. The increase in the number of TH$^+$ interneurons in the OB likely does not arise from simple activation of the TH gene promoter but rather is the result of cell-type switching of neurochemically immature prospective OB interneurons triggered by the loss of $G\alpha_o$.

The increased dopaminergic tone in the OB of *Gnao*$^{-/-}$ mice may reflect a compensatory mechanism triggered by the early defective development of the MOE, which likely interferes with pheromone signal transduction at the level of the GL. Consistent with our in vivo results, the ratio of TH$^+$ neurons to Tubb3$^+$ neurons was also increased in dissociated cell cultures prepared from the OB of E16.5 *Gnao*$^{-/-}$ mice, whereas the ratio of CB$^+$ neurons to Tubb3$^+$ neurons was decreased. Given that TH$^+$ and CB$^+$ neurons originate from a common progenitor pool in the dorsal lateral ganglionic eminence during the embryonic period and CR$^+$ neurons are derived from progenitor cells located elsewhere (38), it is likely that the reciprocal changes in the number of TH$^+$ cells and CB$^+$ cells in the OB of *Gnao*$^{-/-}$ mice are attributable to altered cell-type specification rather than to

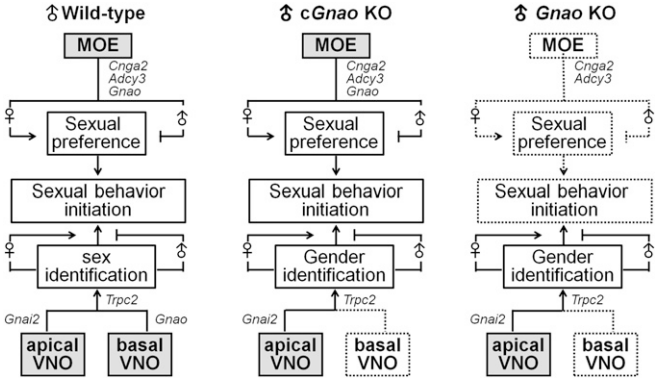

Fig. 6. Model for the roles of the VNO and MOE in the response of male mice to pheromones. Pheromones are detected in the MOE and VNO and evoke social (intermale and maternal aggression) and sexual behaviors. Deletion of *Trpc2* disrupts aggressive behavior while sparing mating behavior (3, 4). Deletion of MOE-specific genes, such as *Cnga2* or *Adcy3*, abrogates preference for the opposite sex and mating behavior (8, 9). Deletion of *Gnai2*, which is expressed in the apical VNO and anterior AOB, disrupts aggressive behavior without affecting preference for the opposite sex (12). Deletion of *Gnao* in the basal VNO and posterior AOB (c*Gnao* KO) disrupts aggressiveness while sparing mating behavior (13, 14). In the present study, deletion of *Gnao* in the MOE and VNO (*Gnao* KO) resulted in a loss of both preference for the opposite sex and mating behavior. In relaying pheromone signals to the brain, the MOE may contribute more to the preference for the opposite sex, and the VNO may contribute more to gender identification.

the induction of TH expression or enhanced survival of TH^+ neurons. Further studies are necessary to elucidate how G_o regulates the expression of intrinsic transcription factors that specify the phenotype of these various interneurons.

Although the binding of a variety of neurotransmitters to cognate receptors is thought to trigger G_o signaling, the functions of $G\alpha_o$ in the brain remain largely unknown, partly because of the high mortality and severe neurological phenotypes of *Gnao*$^{-/-}$ mice (15). We now provide evidence that G_o regulates adult neurogenesis and neuronal survival in the MOE and contributes to cell-type specification of OB interneurons. Our results may provide a basis for the identification of pheromone receptors in the MOE.

Materials and Methods

Standard procedures and methods were used for histological analysis, immunohistochemistry, in situ hybridization, TUNEL staining, and statistical analyses. $P < 0.05$ was considered statistically significant. Expanded methods and materials are available in *SI Materials and Methods*.

Mice. *Gnao*$^{-/-}$ and *Gnao*$^{+/+}$ littermate mice were obtained by interbreeding *Gnao*$^{+/-}$ littermates. Adult male mice were used for all experiments and analyses unless indicated otherwise. All experimental procedures were reviewed and approved by the Institutional Animal Research Ethics Committee of Ajou University and by the National Institute of Environmental Health Sciences.

Food-Detection Test. The food-detection test was performed in a clear, closed acrylic chamber with a black box attached on each side. Food pellets were hidden in only one of the black boxes. The mouse was deprived of food for 1 d and was placed at the midline of the chamber. Behavior was recorded for 10 min under red-light illumination, and the time required for the mouse to locate the food-containing box and the total time spent near the food were determined. Each mouse was subjected to three trials.

Male Sexual Behavior Test. The male sexual behavior test was performed in a clean cage into which a male mouse was placed. An estrous female mouse, prepared as previously described (39), was introduced into the test cage, and the sexual behavior of the male was recorded for 1 h under red-light illumination.

Soiled Bedding Test. The soiled bedding preference test was performed as previously described (40). Each animal was subjected to three trials performed on the same day, with the three compartments containing soiled bedding being arranged randomly to eliminate the influence of positional preference.

OB Primary Neuron Culture. OB primary neuron cultures were prepared from E16.5 embryos as previously described (41).

ACKNOWLEDGMENTS. We thank Dr. Jaesang Kim (Ewha Womans University) and Dr. Joong-Jean Park (Korea University) for discussions and comments on the manuscript and Dr. Ronald Herbert (National Institute of Environmental Health Sciences) for help with histology. This study was supported by Bio & Medical Technology Development Program of the Korean National Research Foundation Grants NRF-2013M3C7A1056565 and NRF-2015M3A9B4067067 (to H.S.-K.) and by NIH Intramural Research Program Grant Z01-ES101643 (to L.B.).

1. Clancy AN, Coquelin A, Macrides F, Gorski RA, Noble EP (1984) Sexual behavior and aggression in male mice: Involvement of the vomeronasal system. *J Neurosci* 4(9):2222–2229.
2. Kim S, et al. (2012) Paradoxical contribution of SK3 and GIRK channels to the activation of mouse vomeronasal organ. *Nat Neurosci* 15(9):1236–1244.
3. Stowers L, Holy TE, Meister M, Dulac C, Koentges G (2002) Loss of sex discrimination and male-male aggression in mice deficient for TRP2. *Science* 295(5559):1493–1500.
4. Leypold BG, et al. (2002) Altered sexual and social behaviors in trp2 mutant mice. *Proc Natl Acad Sci USA* 99(9):6376–6381.
5. Petrulis A, Peng M, Johnston RE (1999) Effects of vomeronasal organ removal on individual odor discrimination, sex-odor preference, and scent marking by female hamsters. *Physiol Behav* 66(1):73–83.
6. Pankevich DE, Baum MJ, Cherry JA (2004) Olfactory sex discrimination persists, whereas the preference for urinary odorants from estrous females disappears in male mice after vomeronasal organ removal. *J Neurosci* 24(42):9451–9457.
7. Keller M, Douhard Q, Baum MJ, Bakker J (2006) Sexual experience does not compensate for the disruptive effects of zinc sulfate–lesioning of the main olfactory epithelium on sexual behavior in male mice. *Chem Senses* 31(8):753–762.
8. Mandiyan VS, Coats JK, Shah NM (2005) Deficits in sexual and aggressive behaviors in Cnga2 mutant mice. *Nat Neurosci* 8(12):1660–1662.
9. Wang Z, et al. (2006) Pheromone detection in male mice depends on signaling through the type 3 adenylyl cyclase in the main olfactory epithelium. *J Neurosci* 26(28):7375–7379.
10. Belluscio L, Gold GH, Nemes A, Axel R (1998) Mice deficient in G(olf) are anosmic. *Neuron* 20(1):69–81.
11. Wekesa KS, Anholt RR (1999) Differential expression of G proteins in the mouse olfactory system. *Brain Res* 837(1-2):117–126.
12. Norlin EM, Gussing F, Berghard A (2003) Vomeronasal phenotype and behavioral alterations in G alpha i2 mutant mice. *Curr Biol* 13(14):1214–1219.
13. Chamero P, et al. (2011) G protein G(alpha)o is essential for vomeronasal function and aggressive behavior in mice. *Proc Natl Acad Sci USA* 108(31):12898–12903.
14. Oboti L, et al. (2014) A wide range of pheromone-stimulated sexual and reproductive behaviors in female mice depend on G protein Gαo. *BMC Biol* 12:31.
15. Jiang M, et al. (1998) Multiple neurological abnormalities in mice deficient in the G protein Go. *Proc Natl Acad Sci USA* 95(6):3269–3274.
16. Lee SJ, et al. (2008) The vomeronasal organ and adjacent glands express components of signaling cascades found in sensory neurons in the main olfactory system. *Mol Cells* 26(5):503–513.
17. Tanaka M, Treloar H, Kalb RG, Greer CA, Strittmatter SM (1999) G(o) protein-dependent survival of primary accessory olfactory neurons. *Proc Natl Acad Sci USA* 96(24):14106–14111.
18. Kam JW, Raja R, Cloutier JF (2014) Cellular and molecular mechanisms regulating embryonic neurogenesis in the rodent olfactory epithelium. *Int J Dev Neurosci* 37:76–86.
19. Ying N, et al. (2012) Progress in defining heterogeneity and modeling periglomerular cells in the olfactory bulb. *Sci China Life Sci* 55(7):567–575.
20. Baker H, Morel K, Stone DM, Maruniak JA (1993) Adult naris closure profoundly reduces tyrosine hydroxylase expression in mouse olfactory bulb. *Brain Res* 614(1-2):109–116.
21. Liu N, et al. (1999) Unique regulation of immediate early gene and tyrosine hydroxylase expression in the odor-deprived mouse olfactory bulb. *J Biol Chem* 274(5):3042–3047.
22. Sawada M, et al. (2011) Sensory input regulates spatial and subtype-specific patterns of neuronal turnover in the adult olfactory bulb. *J Neurosci* 31(32):11587–11596.
23. Jiang M, Spicher K, Boulay G, Wang Y, Birnbaumer L (2001) Most central nervous system D2 dopamine receptors are coupled to their effectors by Go. *Proc Natl Acad Sci USA* 98(6):3577–3582.
24. Vergaño-Vera E, et al. (2006) Generation of GABAergic and dopaminergic interneurons from endogenous embryonic olfactory bulb precursor cells. *Development* 133(21):4367–4379.
25. Munger SD, Leinders-Zufall T, Zufall F (2009) Subsystem organization of the mammalian sense of smell. *Annu Rev Physiol* 71:115–140.
26. Touhara K, Vosshall LB (2009) Sensing odorants and pheromones with chemosensory receptors. *Annu Rev Physiol* 71:307–332.
27. Kuhlmann K, et al. (2014) The membrane proteome of sensory cilia to the depth of olfactory receptors. *Mol Cell Proteomics* 13(7):1828–1843.
28. Luo AH, et al. (2002) Impaired olfactory behavior in mice deficient in the alpha subunit of G(o). *Brain Res* 941(1-2):62–71.
29. Sternson SM, Nicholas Betley J, Cao ZF (2013) Neural circuits and motivational processes for hunger. *Curr Opin Neurobiol* 23(3):353–360.
30. Scholz P, et al. (2016) Transcriptome analysis of murine olfactory sensory neurons during development using single cell RNA-Seq. *Chem Senses* 41(4):313–323.
31. Scholz P, et al. (2016) Identification of a novel Gnao-mediated alternate olfactory signaling pathway in murine OSNs. *Front Cell Neurosci* 10:63.
32. Wong ST, et al. (2000) Disruption of the type III adenylyl cyclase gene leads to peripheral and behavioral anosmia in transgenic mice. *Neuron* 27(3):487–497.
33. Liberles SD, Buck LB (2006) A second class of chemosensory receptors in the olfactory epithelium. *Nature* 442(7103):645–650.
34. Juilfs DM, et al. (1997) A subset of olfactory neurons that selectively express cGMP-stimulated phosphodiesterase (PDE2) and guanylyl cyclase-D define a unique olfactory signal transduction pathway. *Proc Natl Acad Sci USA* 94(7):3388–3395.
35. Omura M, Mombaerts P (2014) Trpc2-expressing sensory neurons in the main olfactory epithelium of the mouse. *Cell Reports* 8(2):583–595.
36. Mundiñano IC, et al. (2011) Increased dopaminergic cells and protein aggregates in the olfactory bulb of patients with neurodegenerative disorders. *Acta Neuropathol* 122(1):61–74.
37. Ross GW, et al. (2008) Association of olfactory dysfunction with risk for future Parkinson's disease. *Ann Neurol* 63(2):167–173.
38. Kohwi M, et al. (2007) A subpopulation of olfactory bulb GABAergic interneurons is derived from Emx1- and Dlx5/6-expressing progenitors. *J Neurosci* 27(26):6878–6891.
39. Choi CI, et al. (2008) Effects of estrogen on lifespan and motor functions in female hSOD1 G93A transgenic mice. *J Neurol Sci* 268(1-2):40–47.
40. Portillo W, Paredes RG (2004) Sexual incentive motivation, olfactory preference, and activation of the vomeronasal projection pathway by sexually relevant cues in noncopulating and naive male rats. *Horm Behav* 46(3):330–340.
41. Iacovitti L, Evinger MJ, Stull ND (1992) Muscle-derived differentiation factor increases expression of the tyrosine hydroxylase gene and enzyme activity in cultured dopamine neurons from the rat midbrain. *Brain Res Mol Brain Res* 16(3-4):215–222.
42. Ishii T, Hirota J, Mombaerts P (2003) Combinatorial coexpression of neural and immune multigene families in mouse vomeronasal sensory neurons. *Curr Biol* 13(5):394–400.